

November 6, 2018

Reconstructing the Higgs boson in dileptonic W decays at hadron collider

Kiwoon Choi^a, Suyong Choi^b, Jae Sik Lee^c, Chan Beom Park^a

^a*Department of Physics, KAIST, Daejeon 305-701, Korea*

^b*Sungkyunkwan University, Suwon 440-746, Korea*

^c*Physics Division, National Center for Theoretical Sciences, Hsinchu, Taiwan*

ABSTRACT

We examine the prospect to measure the Higgs boson mass using the recently introduced kinematic variable, the M_{T2} -Assisted On-Shell (MAOS) momentum, that provides a systematic approximation to the invisible neutrino momenta in dileptonic decays of W -boson pair. For this purpose, we introduce a modified version of the MAOS momentum, that is applicable even when one or both of the W -bosons from the Higgs decay are in off-shell. It is demonstrated that the MAOS Higgs mass distribution, constructed with the MAOS neutrino momenta, shows a clear peak at the true Higgs boson mass when an event cut selecting higher value of M_{T2} is employed. We perform the likelihood analysis for this MAOS mass distribution to determine the Higgs boson mass, and find it can improve the accuracy of the Higgs mass measurement. Our results indicate that the MAOS Higgs mass can be useful also for the discovery or exclusion of the Higgs boson in certain mass range.

1 Introduction

Hunting down the Higgs boson, the last ingredient of the Standard Model (SM), is one of the most important tasks of the LHC [1, 2]. The LEP experiments established a lower bound of 114.4 GeV, at 95% confidence level, on the mass of the SM Higgs boson [3]. On the other hand, the electroweak precision data points towards a relatively light SM Higgs boson with $m_H \lesssim 185$ GeV at 95% confidence level [4]. Recently, Tevatron data have excluded the SM Higgs mass in the range $160 \text{ GeV} \leq m_H \leq 170 \text{ GeV}$ again at 95% confidence level [5].

The strategy for the Higgs boson search depends on its decay pattern. The SM Higgs boson lighter than about 180 GeV mainly decays into the b quarks and W bosons. At hadron collider such as the Tevatron or the LHC, Higgs boson search through the b quark channel appears to be very difficult due to overwhelming QCD backgrounds. In this respect, the Higgs decay $H \rightarrow WW \rightarrow l\nu l'\nu'$ with $l, l' = e, \mu$ may provide the best search channel for the SM Higgs boson in the mass range $135 \text{ GeV} \leq m_H \leq 180 \text{ GeV}$. Even for a heavier Higgs boson with $m_H \gtrsim 2M_Z$, this channel gets benefit from a larger branching ratio compared to the decay $H \rightarrow ZZ \rightarrow 4l$. A drawback is that this channel involves two invisible neutrinos, making it impossible to reconstruct the Higgs boson mass directly. One then has to rely on a Higgs-induced excess in the distribution of certain observables, and this procedure typically requires an accurate estimate of the background contributions [6].

Recently, a new collider variable, the M_{T2} -Assisted On-Shell (MAOS) momentum, has been introduced [7] to approximate the invisible particle momenta in the process $XX' \rightarrow V\chi V'\chi'$, where X and X' denote pair-produced mother particles, V and V' represent the visible particles (one or more particles for each of them) produced by the decays of X and X' , respectively, and χ and χ' are the invisible particles having the same mass. In this paper, we examine the possibility to determine the Higgs boson mass using the MAOS momenta of neutrinos in the process $H \rightarrow WW \rightarrow l\nu l'\nu'$. An interesting feature of this approach is that one can use the collider variable M_{T2} [8] for event selection, which enhances both the signal to background ratio and the efficiency of the MAOS momentum approximation to the true neutrino momentum*. As we will see, the MAOS Higgs mass distribution, constructed with the MAOS neutrino momenta under a suitable M_{T2} cut, shows a clear peak over the background at the true Higgs boson mass. One can then determine the true Higgs boson mass by performing the likelihood fit to the MAOS Higgs mass distribution. The results of our likelihood analysis indicate that the precision can be significantly improved when the MAOS Higgs momentum is used for the Higgs mass determination, possibly combined with the kinematic variables considered in [1, 10, 11]. One can do a similar likelihood analysis for the Higgs boson discovery or exclusion, which might enhance the significance of the result for certain range of the Higgs boson mass.

*It has been pointed out recently that M_{T2} can be used also for the selection of new physics events [9].

2 M_{T2} -assisted on-shell (MAOS) momentum

In this section, we discuss some features of the MAOS momentum for the dileptonic Higgs boson decay:

$$H \rightarrow W(p+k)W(q+l) \rightarrow l(p) \nu(k) l'(q) \nu'(l). \quad (1)$$

For the sake of discussion, we decompose the final state momenta into the transverse and longitudinal parts as follows:

$$\begin{aligned} p^\mu &= (\sqrt{|\mathbf{p}_T|^2 + p_L^2}, \mathbf{p}_T, p_L), & k^\mu &= (\sqrt{|\mathbf{k}_T|^2 + k_L^2}, \mathbf{k}_T, k_L), \\ q^\mu &= (\sqrt{|\mathbf{q}_T|^2 + q_L^2}, \mathbf{q}_T, q_L), & l^\mu &= (\sqrt{|\mathbf{l}_T|^2 + l_L^2}, \mathbf{l}_T, l_L), \end{aligned} \quad (2)$$

where we have neglected the masses of the charged leptons and neutrinos. For a Higgs boson mass $m_H \geq 2M_W$, the two W bosons are in on-shell. On the other hand, if $m_H < 2M_W$, one or both of W bosons should be in off-shell. Regardless of whether the W bosons are in on-shell or not, one can construct the event-by-event variable M_{T2} [8] which is given by[†]

$$M_{T2} \equiv \min_{\mathbf{k}_T + \mathbf{l}_T = \cancel{\mathbf{p}}_T} \left[\max \left\{ M_T^{(1)}, M_T^{(2)} \right\} \right], \quad (3)$$

where $\cancel{\mathbf{p}}_T$ denotes the missing transverse momentum carried by neutrinos, and $M_T^{(1),(2)}$ are the transverse masses of the two decaying W bosons, which are given by

$$\left(M_T^{(1)} \right)^2 = 2 (|\mathbf{p}_T| |\mathbf{k}_T| - \mathbf{p}_T \cdot \mathbf{k}_T), \quad \left(M_T^{(2)} \right)^2 = 2 (|\mathbf{q}_T| |\mathbf{l}_T| - \mathbf{q}_T \cdot \mathbf{l}_T). \quad (4)$$

If the Higgs boson is produced without having a sizable transverse momentum, so that the W -pair transverse momentum $\mathbf{p}_T^{WW} \approx 0$, the missing transverse momentum is (approximately) given by

$$\cancel{\mathbf{p}}_T = -(\mathbf{p}_T + \mathbf{q}_T). \quad (5)$$

In this case, M_{T2} is simply given by [12]

$$M_{T2}^2 = \left(M_T^{(1)} \right)^2 = \left(M_T^{(2)} \right)^2 = 2 (|\mathbf{p}_T| |\mathbf{q}_T| + \mathbf{p}_T \cdot \mathbf{q}_T). \quad (6)$$

In fact, for both the signal W bosons from $H \rightarrow WW$ and the background W bosons from $q\bar{q} \rightarrow WW$, initial state radiations (ISR) typically give[‡] $|\mathbf{p}_T^{WW}| = 10 \sim 40$ GeV, which would be non-negligible compared to the typical lepton transverse momenta in the final state. Still the above expression of M_{T2} obtained in the limit $\mathbf{p}_T^{WW} = 0$ shows some qualitative feature of M_{T2} for non-negligible \mathbf{p}_T^{WW} , e.g. the correlation between M_{T2} and the transverse opening angle $\Delta\Phi_u$ between \mathbf{p}_T and \mathbf{q}_T . In the following, ISR effects will be fully included in the numerical evaluation of M_{T2} and the MAOS momentum.

[†]For recent applications of M_{T2} to mass determination, see [12–14].

[‡]Typically the signal has a slightly larger \mathbf{p}_T^{WW}

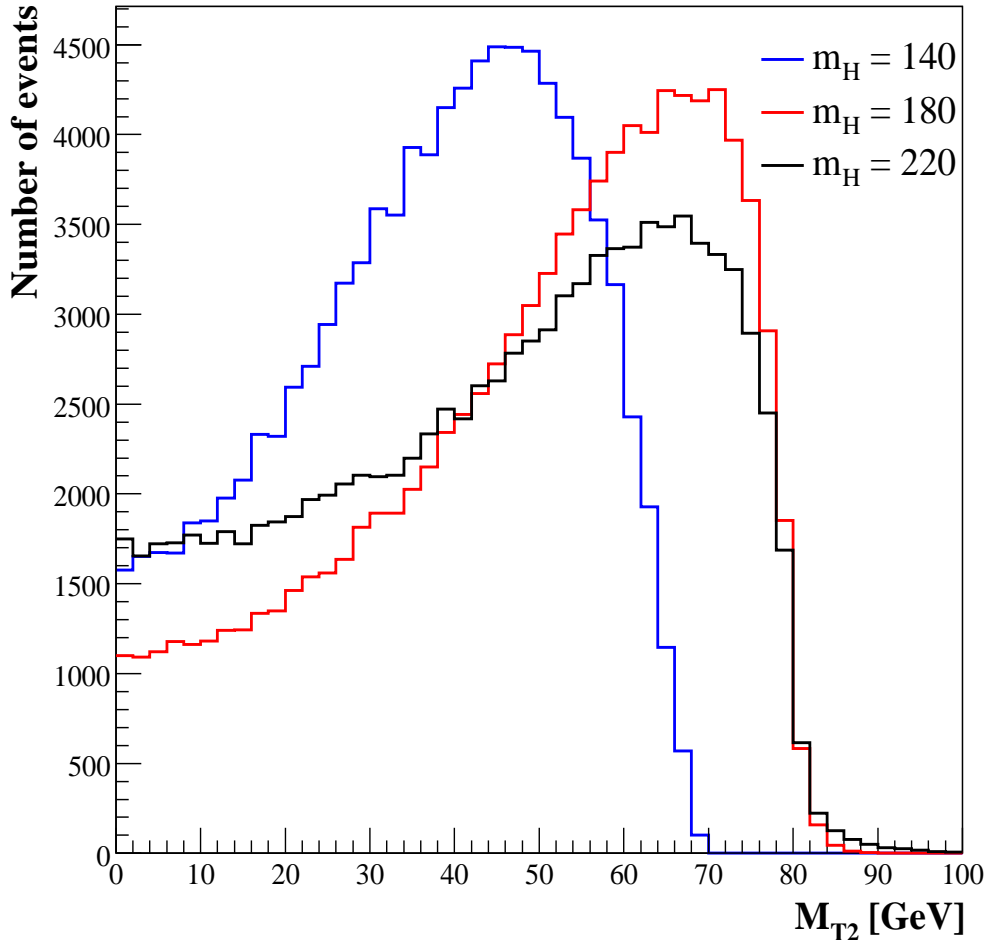


Figure 1: *The distributions of M_{T2} for various values of m_H .*

As the transverse mass is bounded above by the invariant mass, the above relation implies

$$M_{T2} \leq \min(M^{(1)}, M^{(2)}) \leq \frac{m_H}{2}, \quad (7)$$

where $M^{(1),(2)}$ are the invariant masses of the intermediate W bosons. One then immediately finds that the M_{T2} of dileptonic Higgs decay is bounded as (upon ignoring the finite decay widths of the Higgs and W bosons)

$$M_{T2} \leq \min(M_W, \frac{m_H}{2}). \quad (8)$$

In Fig. 1, we depict the M_{T2} distribution for several different values of m_H , where the event

set is generated for the process $gg \rightarrow H \rightarrow WW \rightarrow l\nu l'\nu'$ at the LHC beam condition[§]. The results show that the endpoint value is indeed $m_H/2$ for $m_H < 2M_W$, while it is M_W for $m_H > 2M_W$.

The MAOS momenta [7] are the four-vector variables which approximate the momenta of invisible particles in collider event of the type

$$X(p+k)X'(q+l) \rightarrow V(p) + \chi(k) + V'(q) + \chi'(l),$$

where X and X' denote pair-produced (not necessarily identical and not necessarily in on-shell) mother particles, $V(p)$ and $V'(q)$ represent (one or more) visible particles with total momenta p and q , which are produced by the decays of X and X' , respectively, and χ and χ' are two invisible particles having the same mass. The transverse MAOS momenta are defined as the trial transverse momenta of χ and χ' that determine the M_{T2} of the event, i.e. \mathbf{k}_T and \mathbf{l}_T minimizing $\max\{M_T(X), M_T(X')\}$ under the constraint $\mathbf{k}_T + \mathbf{l}_T = \mathbf{p}'_T$, where $M_T(X)$ and $M_T(X')$ are the transverse masses of X and X' , respectively. For the process $WW \rightarrow l(p)\nu(k)l'(q)\nu'(l)$, the transverse MAOS momenta are uniquely determined by the conditions

$$\begin{aligned} M_{T2}(\mathbf{p}_T, \mathbf{q}_T, \mathbf{p}'_T) &= \sqrt{2(|\mathbf{p}_T||\mathbf{k}_T^{\text{maos}}| - \mathbf{p}_T \cdot \mathbf{k}_T^{\text{maos}})} \\ &= \sqrt{2(|\mathbf{q}_T||\mathbf{l}_T^{\text{maos}}| - \mathbf{q}_T \cdot \mathbf{l}_T^{\text{maos}})}, \\ \mathbf{p}'_T &= \mathbf{k}_T^{\text{maos}} + \mathbf{l}_T^{\text{maos}}. \end{aligned} \quad (9)$$

For an event without initial state radiation, i.e. an event with $\mathbf{p}_T^{WW} = 0$, we have $\mathbf{p}'_T = -(\mathbf{p}_T + \mathbf{q}_T)$ and M_{T2} given by (6). In this case, the transverse MAOS momenta are simply given by

$$\mathbf{k}_T^{\text{maos}} = -\mathbf{q}_T, \quad \mathbf{l}_T^{\text{maos}} = -\mathbf{p}_T. \quad (10)$$

There can be two different schemes to define the longitudinal MAOS momenta. One is to require the on-shell conditions for both the invisible particles in the final state and the mother particles in the intermediate state. In the case of $WW \rightarrow l(p)\nu(k)l'(q)\nu'(l)$, it corresponds to

$$(k_{\text{maos}})^2 = (l_{\text{maos}})^2 = 0, \quad (p + k_{\text{maos}})^2 = (q + l_{\text{maos}})^2 = M_W^2, \quad (11)$$

which results in

$$\begin{aligned} k_L^{\text{maos}}(\pm) &= \frac{1}{|\mathbf{p}_T|^2} \left[p_L A \pm \sqrt{|\mathbf{p}_T|^2 + p_L^2} \sqrt{A^2 - |\mathbf{p}_T|^2 |\mathbf{k}_T^{\text{maos}}|^2} \right], \\ l_L^{\text{maos}}(\pm) &= \frac{1}{|\mathbf{q}_T|^2} \left[q_L B \pm \sqrt{|\mathbf{q}_T|^2 + q_L^2} \sqrt{B^2 - |\mathbf{q}_T|^2 |\mathbf{l}_T^{\text{maos}}|^2} \right], \end{aligned} \quad (12)$$

[§]For the analysis in this section, we do not include the effects of hadronization and detector smearing, while those effects are incorporated in the analysis of the next section.

where $A \equiv M_W^2/2 + \mathbf{p}_T \cdot \mathbf{k}_T^{\text{maos}}$ and $B \equiv M_W^2/2 + \mathbf{q}_T \cdot \mathbf{l}_T^{\text{maos}}$. Note that the above longitudinal MAOS momenta have four-fold degeneracy for each event (two-fold degeneracy for each neutrino MAOS momentum). Another possible scheme is to require

$$(k_{\text{maos}})^2 = (l_{\text{maos}})^2 = 0, \quad (p + k_{\text{maos}})^2 = (q + l_{\text{maos}})^2 = M_{T2}^2, \quad (13)$$

which gives unique longitudinal MAOS momenta as

$$k_L^{\text{maos}} = \frac{|\mathbf{k}_T^{\text{maos}}|}{|\mathbf{p}_T|} p_L, \quad l_L^{\text{maos}} = \frac{|\mathbf{l}_T^{\text{maos}}|}{|\mathbf{q}_T|} q_L. \quad (14)$$

To distinguish these two schemes, the MAOS momenta of (10) and (12) will be called the original MAOS momenta as they are the one originally defined in [7], while (10) and (14) will be called the modified MAOS momenta.

A nice feature of the MAOS momenta is that they provide a systematic approximation to the invisible particle momenta [7], i.e. the neutrino momenta in our case. For the case of $m_H > 2M_W$, both of the two W bosons in $H \rightarrow W^+W^-$ are on mass-shell, and then the endpoint value of M_{T2} is given by M_W . In this case, one easily finds that both the original MAOS momenta and the modified MAOS momenta approach to the true neutrino momenta in the limit of the endpoint event with $M_{T2} = M_W$. (Note that $k_L^{\text{maos}(+)} = k_L^{\text{maos}(-)}$ for the endpoint event.) For generic events with $M_{T2} < M_W$, the MAOS momenta generically differ from the true neutrino momenta. Even in these cases, we can infer from its distribution that the MAOS momentum provide a reasonable approximation to the true neutrino momentum. As the approximation gets better for larger value of M_{T2} , one can systematically improve the efficiency of approximation with M_{T2} cut.

In Fig. 2, we show the distributions of the difference between the MAOS momentum and the true neutrino momentum,

$$\Delta k_{T,L} = k_{T,L}^{\text{true}} - k_{T,L}^{\text{maos}},$$

for $m_H = 180$ GeV and $m_H = 140$ GeV, respectively. The left panels include the distributions of the full event set for $gg \rightarrow H \rightarrow WW \rightarrow l\nu l'\nu'$ generated at the LHC condition, while the right panels show the distributions of the top 10% subset near the endpoint of M_{T2} . By definition, the original and modified MAOS schemes give the same transverse MAOS momenta, thus the same Δk_T distribution (black). For Δk_L in the original MAOS scheme, we construct its distribution using the two solutions $\{k_L^{\text{maos}(+)}, l_L^{\text{maos}(+)}\}$ and $\{k_L^{\text{maos}(-)}, l_L^{\text{maos}(-)}\}$ for each event. For $m_H > 2M_W$, our results indicate that the original scheme (red) is a bit better than the modified scheme (blue), if one considers the full event set. However, the two schemes show similar performance if one employs a proper M_{T2} cut, say a cut selecting about 30% of the near-endpoint events. Both the modified and original schemes recover the true neutrino momentum for the exact endpoint event with $M_{T2} = M_W$. On the other hand, when $m_H < 2M_W$ so that one or both W -bosons

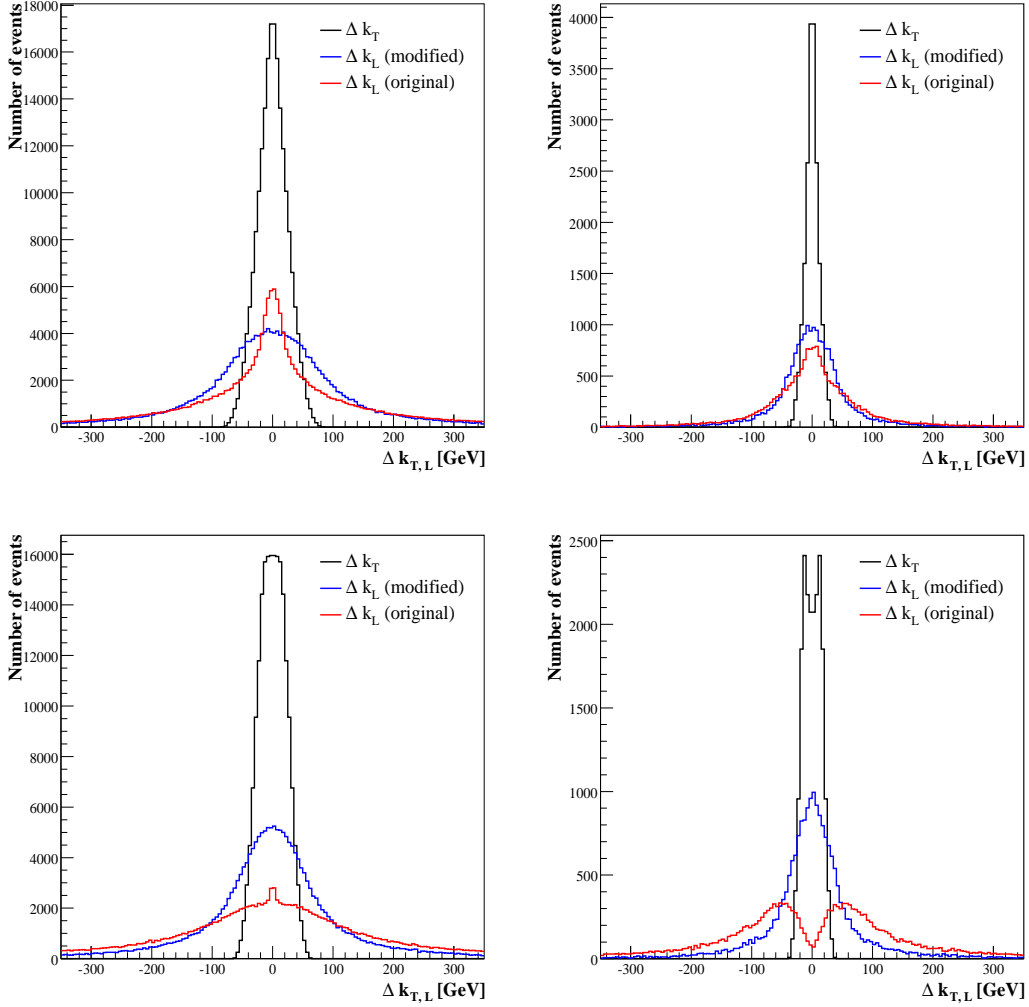


Figure 2: Distributions of $\Delta k_T = k_T^{\text{true}} - k_T^{\text{maos}}$ (black), Δk_L for the original MAOS momenta (red), and Δk_L for the modified MAOS momenta (blue). The upper frames are for $m_H = 180$ GeV, and the lower frames are for $m_H = 140$ GeV. Full event set is used for the left frames, while the top 10% near endpoint events of M_{T_2} are used for the right frames.

are in off-shell, the modified MAOS is clearly the better choice to approximate the neutrino momenta. For off-shell W , the original MAOS scheme does not give correct neutrino momenta even for the endpoint event of M_{T_2} , while the modified MAOS scheme does.

Once the MAOS momenta of neutrinos are obtained, one can construct the MAOS Higgs mass:

$$(m_H^{\text{maos}})^2 \equiv (p + k_{\text{maos}} + q + l_{\text{maos}})^2. \quad (15)$$

A nice feature of m_H^{maos} is that its distribution has a peak at the true Higgs boson mass, which becomes narrower under a stronger M_{T_2} cut. In Fig. 3, we show the MAOS Higgs

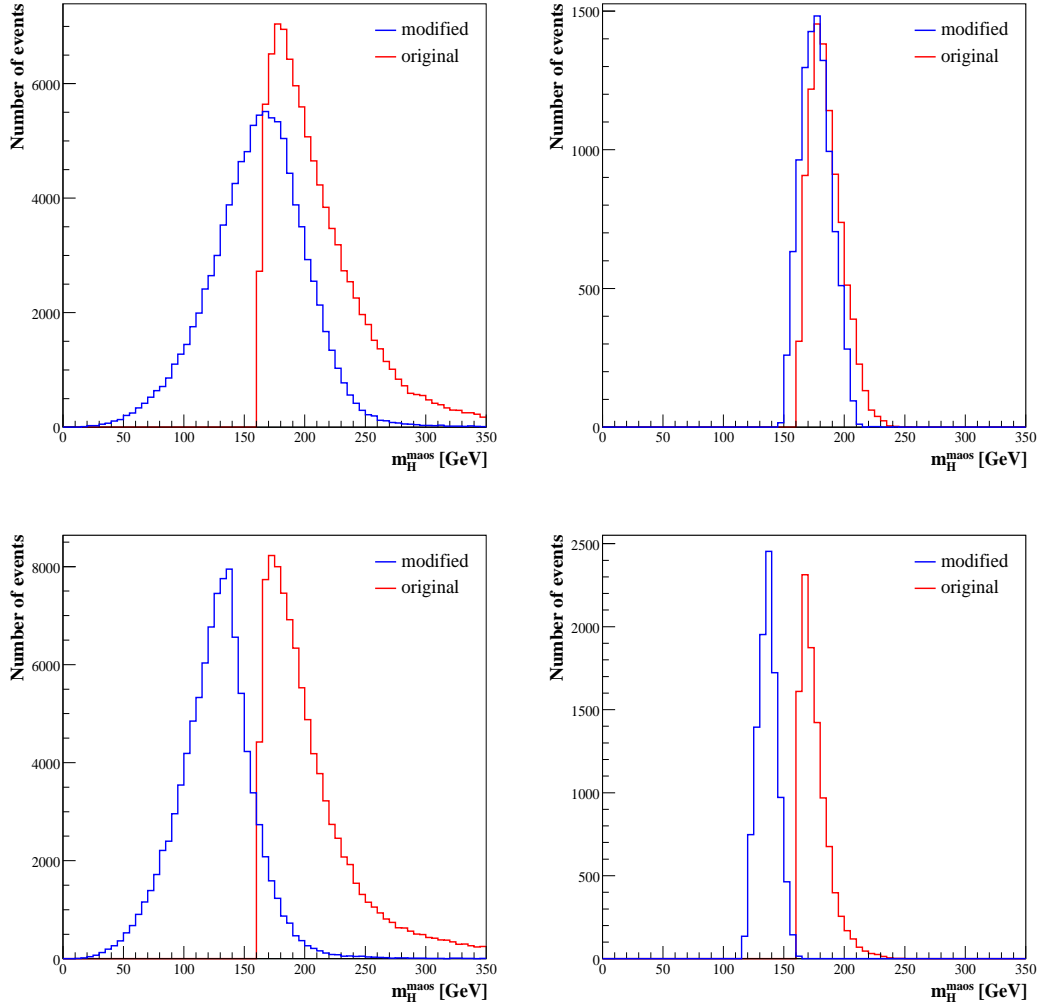


Figure 3: *The MAOS Higgs mass distributions for the full event set (left frames) and the top 10 % near endpoint events of M_{T2} (right frames) in the original (red) and modified (blue) MAOS schemes. The upper frames are for $m_H = 180$ GeV and the lower frames are for $m_H = 140$ GeV.*

mass distributions of the full event set (left panel) of $gg \rightarrow H \rightarrow WW \rightarrow \nu l' \nu'$ generated for $m_H = 180$ and 140 GeV at the LHC condition, and also of the top 10% near endpoint events of M_{T2} (right panel), for both the original MAOS scheme (red) and the modified MAOS scheme (blue). Our results suggest that the modified MAOS scheme can provide a good approximation to the invisible neutrino momenta for both $m_H < 2M_W$ and $m_H > 2M_W$, under a suitable M_{T2} cut selecting near endpoint events. In fact, such an M_{T2} cut is useful in another sense as it enhances the signal to background ratio. As is well known, the dileptons from the Higgs decay are likely to have smaller opening angle than the background, which

is essentially due to that the Higgs boson is a spin zero particle. Then, the expression (6) of M_{T2} indicates that the dileptons from the Higgs decay are likely to have larger M_{T2} than the background because of the same reason.

In the next section, we will perform the likelihood analysis for the MAOS Higgs mass distribution to determine the true Higgs boson mass, while including some of the main backgrounds as well as the detector effects. We will use the modified MAOS scheme since the original MAOS scheme does not work for the case of $m_H < 2M_W$, while the modified MAOS scheme works well for both $m_H < 2M_W$ and $m_H > 2M_W$.

3 MAOS reconstruction of the Higgs boson mass

To investigate the experimental performance of the MAOS reconstruction of the Higgs boson mass at the LHC, we use the PYTHIA6.4 Monte Carlo (MC) generator at NLO [15]. The generated events have been further processed through the fast detector simulation program PGS4 [16] to incorporate the detector effects with reasonable efficiencies and fake rates [17]. Assuming the integrated luminosity of 10 fb^{-1} , we have generated the MC event samples of the SM Higgs boson signal and the two main backgrounds. For the signal, we consider the Higgs boson production via the gluon fusion: $gg \rightarrow H$. For the Higgs mass range $130 \text{ GeV} \lesssim m_H \lesssim 200 \text{ GeV}$, the produced Higgs boson decays mainly into a pair of W bosons. We take into account all the dileptonic decay channels of the W bosons to enhance the signal, $W \rightarrow l\nu$ with $l = e, \mu$. The dominant background comes from the continuum $q\bar{q}, gg \rightarrow WW \rightarrow l\nu l'\nu'$ process, and we include also the $t\bar{t}$ background in which the two top quarks decay into a pair of W bosons and two b jets.

Following [1], we have imposed the following basic selection cuts on the Higgs signal and the backgrounds:

- Require that the event has exactly two isolated, opposite-sign leptons (electron or muon) with $p_T > 15 \text{ GeV}$ and $|\eta| < 2.5$.
- $12 \text{ GeV} < m_{ll} < 300 \text{ GeV}$.
- $|\cancel{p}_T| > 30 \text{ GeV}$.
- No b jets.
- No jets with $p_T > 20 \text{ GeV}$.

It is well known that the background can be significantly reduced by exploiting the helicity correlation between the charged lepton and its mother W boson. Introducing the transverse opening angle between two charged leptons, $\Delta\Phi_{ll}$, the Higgs signal tends to have

a smaller $\Delta\Phi_{ll}$ than the background, which is essentially due to the fact that the Higgs boson is a spin zero particle. Selecting the events with large value of M_{T2} similarly enhances the signal to background ratio, which can be understood by the correlation between M_{T2} and $\Delta\Phi_{ll}$ in (6). In our case, this M_{T2} cut is particularly useful since it enhances also the accuracy of the MAOS reconstruction of the neutrino momenta as discussed in the previous section. In Fig. 4, we show the scatter plots of M_{T2} and $\Delta\Phi_{ll}$ for the signal (left panel) and the background (right panel), obtained after imposing the above basic selection cuts to the data set for $m_H = 170$ GeV, while including the detector effects. As anticipated, the low $\Delta\Phi_{ll}$ and high M_{T2} region is more populated by the signal events, while the high $\Delta\Phi_{ll}$ and low M_{T2} region by the backgrounds. We can also notice a correlation between $\Delta\Phi_{ll}$ and M_{T2} suggested by (6). Fig. 5 shows the M_{T2} distribution (left panel), again for $m_H = 170$ GeV, of the events with $\Delta\Phi_{ll} \leq 1.6$, and the $\Delta\Phi_{ll}$ distribution (right panel) of the events with $M_{T2} \geq 67$ GeV, where the shaded regions represent the backgrounds. Here, the tail of the M_{T2} distribution beyond M_W is mainly due to the W -boson width. We observe that the signal is more likely to have larger M_{T2} . Furthermore, the right panel of Fig. 5 indicates that the M_{T2} cut can significantly enhance the efficiency of the $\Delta\Phi_{ll}$ cut. We thus introduce two additional cuts:

- $\Delta\Phi_{ll} < \Delta\Phi_{ll}^{\text{cut}}$,
- $M_{T2} > M_{T2}^{\text{cut}}$,

where $\Delta\Phi_{ll}^{\text{cut}}$ and M_{T2}^{cut} are chosen to optimize the Higgs mass measurement using the MAOS mass distribution, and their values for various m_H are listed in Table 1.

Table 1: *The $\Delta\Phi_{ll}$ and M_{T2} cuts for various values of m_H .*

m_H (GeV)	130	140	150	160	170	180	190	200
$\Delta\Phi_{ll}^{\text{cut}}$	1.85	1.70	1.65	1.50	1.60	1.70	1.90	2.05
M_{T2}^{cut} (GeV)	38.0	51.0	57.0	66.0	67.0	68.0	69.5	70.0

In Table 2, taking the case of $m_H = 170$ GeV as a specific example, we show how the numbers of signal events and background events are changing under each selection cut. Comparing with the ATLAS cut flows reported in [1], the signal and the dominant WW background are in excellent agreement except for that the overall number of events is somewhat larger in our case[¶]. This may be attributed to the differences in simulating the

[¶]Note that we consider all of the $ee, \mu\mu, e\mu$ events, while [1] included only the $e\mu$ events.

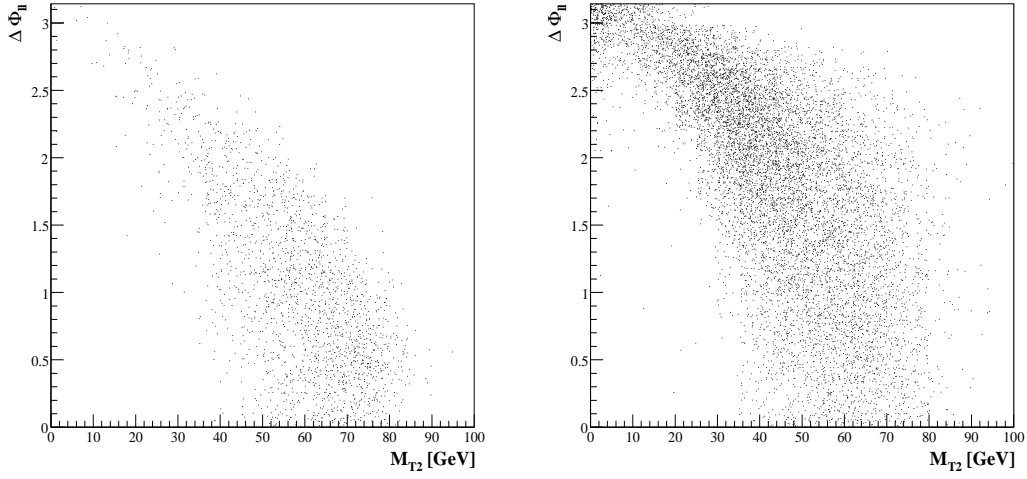


Figure 4: *The scatter plots of M_{T2} and $\Delta\Phi_U$ for the signal (left) and background (right) events after imposing the basic selection cuts. For the signal, $m_H = 170$ GeV is taken.*

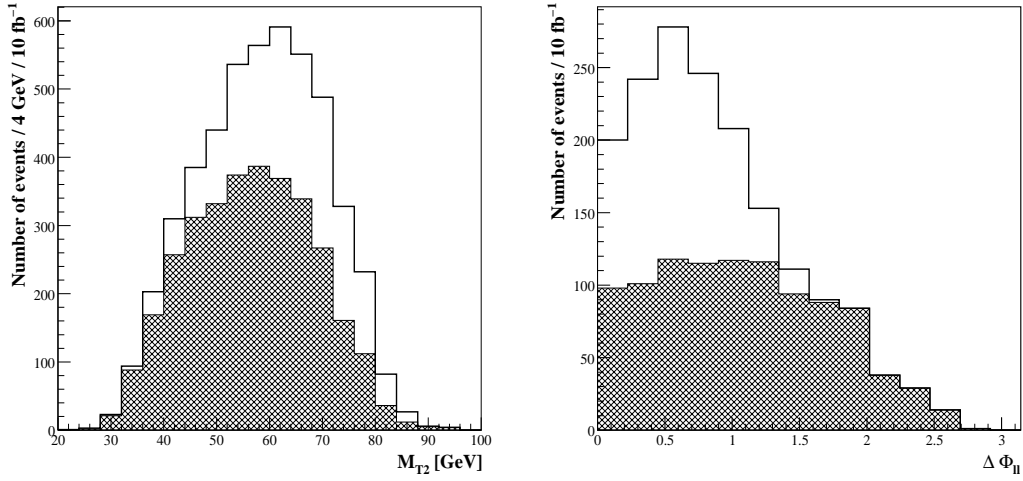


Figure 5: *The M_{T2} distribution (left) for the events with $\Delta\Phi_U < 1.6$, and the $\Delta\Phi_U$ distribution (right) for the events with $M_{T2} > 67$ GeV. Signal events are taken for $m_H = 170$ GeV, and the shaded regions represent the backgrounds.*

jet reconstruction, detector effects and triggering. For the $t\bar{t}$ background, we have a sizable number of events even after imposing the basic selection cuts, but it can be suppressed to a negligible level by the $\Delta\Phi_U$ and M_{T2} cuts.

In Fig. 6, we show the m_H^{maos} distributions for various (nominal) values of the Higgs

Table 2: *Cut flows for $m_H = 170$ GeV with $\Delta\Phi_{ll}^{\text{cut}} = 1.6$ and $M_{T2}^{\text{cut}} = 67$ GeV at 10 fb^{-1} .*

Selection	Selection cuts	$gg \rightarrow H$	WW	$t\bar{t}$
Basic Selection	Lepton selection $+m_{ll}$	4,445	18,501	139,256
	$ \not{p}_T > 30$ GeV	4,012	12,801	120,597
	b -veto	3,956	12,656	60,438
	Jet veto	2,039	8,096	1,287
Tuned Selection	$\Delta\Phi_{ll} < \Delta\Phi_{ll}^{\text{cut}}$	1,621	2,939	332
	$M_{T2} > M_{T2}^{\text{cut}}$	619	585	107

boson mass, obtained by the modified MAOS momenta of neutrinos, while incorporating the M_{T2} and $\Delta\Phi_{ll}$ cuts listed in Table 1. We observe that the modified MAOS scheme is working nicely and each distribution has a clear peak at the true (nominal) Higgs mass independently of whether m_H is below or above $2M_W$.

With the m_H^{maos} distribution constructed as above, we performed a template fitting to determine the Higgs boson mass. Here a template means a simulated distribution with a trial Higgs mass which, in general, is different from the nominal one used to generate the data. For each distribution with the nominal Higgs mass m_H , the 11 templates are generated with the trial Higgs masses between $m_H - 10$ GeV and $m_H + 10$ GeV, in steps of 2 GeV. For example, in each frame of Fig. 6, the solid line shows the template when the trial Higgs mass is the same as the nominal one. Each template is normalized to the corresponding nominal distribution.

The likelihood between a nominal data distribution and a template is defined as the product of individual Poisson probabilities computed in each bin i over the \mathcal{N} bins in the fit range:

$$\mathcal{L} \equiv \prod_i^{\mathcal{N}} \frac{e^{-m_i} m_i^{n_i}}{n_i!}, \quad (16)$$

where n_i and m_i denote the number of events in the i -th bin of the nominal distribution and the normalized template, respectively. In Fig. 7, we show the log likelihood distribution for various Higgs masses in the range between 130 GeV and 200 GeV. The solid line shows the result of a quadratic fitting for each value of m_H . The fitted Higgs boson masses together with $1\text{-}\sigma$ error are listed in Table 3 (see also Fig. 8) for various input Higgs masses, where the $1\text{-}\sigma$ deviated value is defined as the one increasing $-\ln \mathcal{L}$ by $1/2$ [18].

Table 3: *The fitted Higgs boson mass for various input values of m_H at 10 fb^{-1} .*

M_H (GeV)	130	140	150	160	170	180	190	200
Fitted value (GeV)	130.0	140.1	150.9	160.6	170.3	179.4	190.4	199.7
1- σ error (GeV)	2.4	1.7	1.2	1.0	0.9	1.4	2.0	3.5

4 Conclusions

In this paper, we have examined the prospect of measuring the Higgs boson mass using the MAOS neutrino momenta in the Higgs decay $H \rightarrow WW \rightarrow l\nu l\nu$. To optimize the efficiency of the method, we have employed an event selection to combine the well known dilepton azimuthal angle cut, $\Delta\Phi_{ll} < \Delta\Phi_{ll}^{\text{cut}}$, with an M_{T2} cut selecting only the events with $M_{T2} > M_{T2}^{\text{cut}}$. This M_{T2} cut enhances the efficiency of the MAOS momentum approximation to the true neutrino momentum, and the signal to background ratio also. Under such selection, the MAOS Higgs mass distribution constructed with the measured charged lepton momenta and the MAOS neutrino momenta shows a clear peak at the true Higgs boson mass. Likelihood fit analysis for the MAOS Higgs mass distribution suggests that it can provide a precise determination of the Higgs boson mass, and also be useful for the discovery or exclusion of the Higgs boson in certain mass range.

Our analysis can be improved in many respects, e.g. with more extensive study of backgrounds, with more complete detector simulation, and with multi-dimensional fitting including other observables. At the moment, it is not straightforward to compare our results with those of Ref. [1] providing a more complete analysis using the transverse mass variable $M_T^{\text{approx}} = M_T(m_{\nu\nu} = m_{ll})$ (together with $\Delta\Phi_{ll}$ and \mathbf{p}_T^{WW}) instead of the MAOS Higgs mass m_H^{maos} , where $M_T^2 = m_{ll}^2 + m_{\nu\nu}^2 + 2(E_T^l E_T^{\nu\nu} - \mathbf{p}_T^l \cdot \mathbf{p}_T^{\nu\nu})$ denotes the transverse mass of $WW \rightarrow l\nu l\nu$. On the other hand, it is relatively easy to compare our analysis with [10] which discusses the Higgs mass determination with $M_T^{\text{true}} = M_T(m_{\nu\nu} = 0)$ in a simple context including only the dominant background $q\bar{q} \rightarrow WW$ without taking into account the detector effects. Our results appears to be better than (or comparable to) those of [10]. This indicates that incorporating the collider variable m_H^{maos} might improve significantly the accuracy of the Higgs mass measurement, as well as the significance of the Higgs boson discovery or exclusion.

Acknowledgements

We thank W. S. Cho for useful discussions. KC and CBP are supported by the KRF grants funded by the Korean Government (KRF-2007-341-C00010 and KRF-2008-314-C00064), KOSEF grant funded by the Korean Government (No. 2009-0080844), and the BK21 project by the Korean Government. SC is supported by the KRF grant (KRF-2006-331-C00072) and the BK21 project.

References

- [1] G. Aad *et al.* [The ATLAS Collaboration], arXiv:0901.0512 [hep-ex].
- [2] G. L. Bayatian *et al.* [CMS Collaboration], J. Phys. **G34** (2007) 995.
- [3] R. Barate *et al.* [The LEP Working Group for Higgs boson searches, ALEPH, DELPHI, L3, and OPAL Collaborations], Phys. Lett. **B565** (2003) 61 [arXiv:hep-ex/0306033].
- [4] ALEPH, CDF, D0, DELPHI, L3, OPAL, SLD Collaborations, arXiv:0811.4682 [hep-ex].
- [5] CDF Collaboration and D0 Collaboration, arXiv:0903.4001 [hep-ex].
- [6] See, for example, V. Buescher and K. Jakobs, Int. J. Mod. Phys. **A20** (2005) 2523 [arXiv:hep-ph/0504099].
- [7] W. S. Cho, K. Choi, Y. G. Kim and C. B. Park, Phys. Rev. **D79** (2009) 031701 [arXiv:0810.4853 [hep-ph]].
- [8] C. G. Lester and D. J. Summers, Phys. Lett. **B463** (1999) 99 [arXiv:hep-ph/9906349]; A. J. Barr, C. G. Lester and P. Stephens, J. Phys. **G29** (2003) 2343 [arXiv:hep-ph/0304226].
- [9] A. J. Barr and C. Gwenlan, arXiv:0907.2713 [hep-ph].
- [10] A. J. Barr, B. Gripaios and C. G. Lester, arXiv:0902.4864 [hep-ph].
- [11] T. Han, I. W. Kim and J. Song, arXiv:0906.5009 [hep-ph]
- [12] W. S. Cho, K. Choi, Y. G. Kim and C. B. Park, Phys. Rev. Lett. **100** (2008) 171801 [arXiv:0709.0288 [hep-ph]]; W. S. Cho, K. Choi, Y. G. Kim and C. B. Park, JHEP **0802** (2008) 035 [arXiv:0711.4526 [hep-ph]].
- [13] B. Gripaios, JHEP **0802** (2008) 053 [arXiv:0709.2740]; A. J. Barr, B. Gripaios and C. G. Lester, JHEP **0802** (2008) 014 [arXiv:0711.4008].

- [14] M. M. Nojiri, Y. Shimizu, S. Okada, and K. Kawagoe, JHEP **0806** (2008) 035 [arXiv:0802.2412 [hep-ph]]; W. S. Cho, K. Choi, Y. G. Kim and C. B. Park, Phys. Rev. **D78** (2008) 034019 [arXiv:0804.2185 [hep-ph]]; A. J. Barr, G. G. Ross and M. Serna, Phys. Rev. **D78** (2008) 056006 [arXiv:0806.3224 [hep-ph]]; M. M. Nojiri, K. Sakurai, Y. Shimizu and M. Takeuchi, JHEP **0810** (2008) 100 [arXiv:0808.1094 [hep-ph]]; H.-C. Cheng and Z. Han, JHEP **0812** (2008) 063 [arXiv:0810.5178 [hep-ph]]; M. Burns, K. Kong, K. T. Matchev and M. Park, JHEP **0903** (2009) 143 [arXiv:0810.5576 [hep-ph]].
- [15] T. Sjostrand, S. Mrenna and P. Skands, JHEP **0605** (2006) 026 [arXiv:hep-ph/0603175].
- [16] <http://www.physics.ucdavis.edu/~conway/research/software/pgs/pgs4-general.htm>
- [17] See also the talk by J. Conway, http://online.kitp.ucsb.edu/online/lhco_c06/conway/.
- [18] C. Amsler *et al.* [Particle Data Group], Phys. Lett. B **667** (2008) 1.

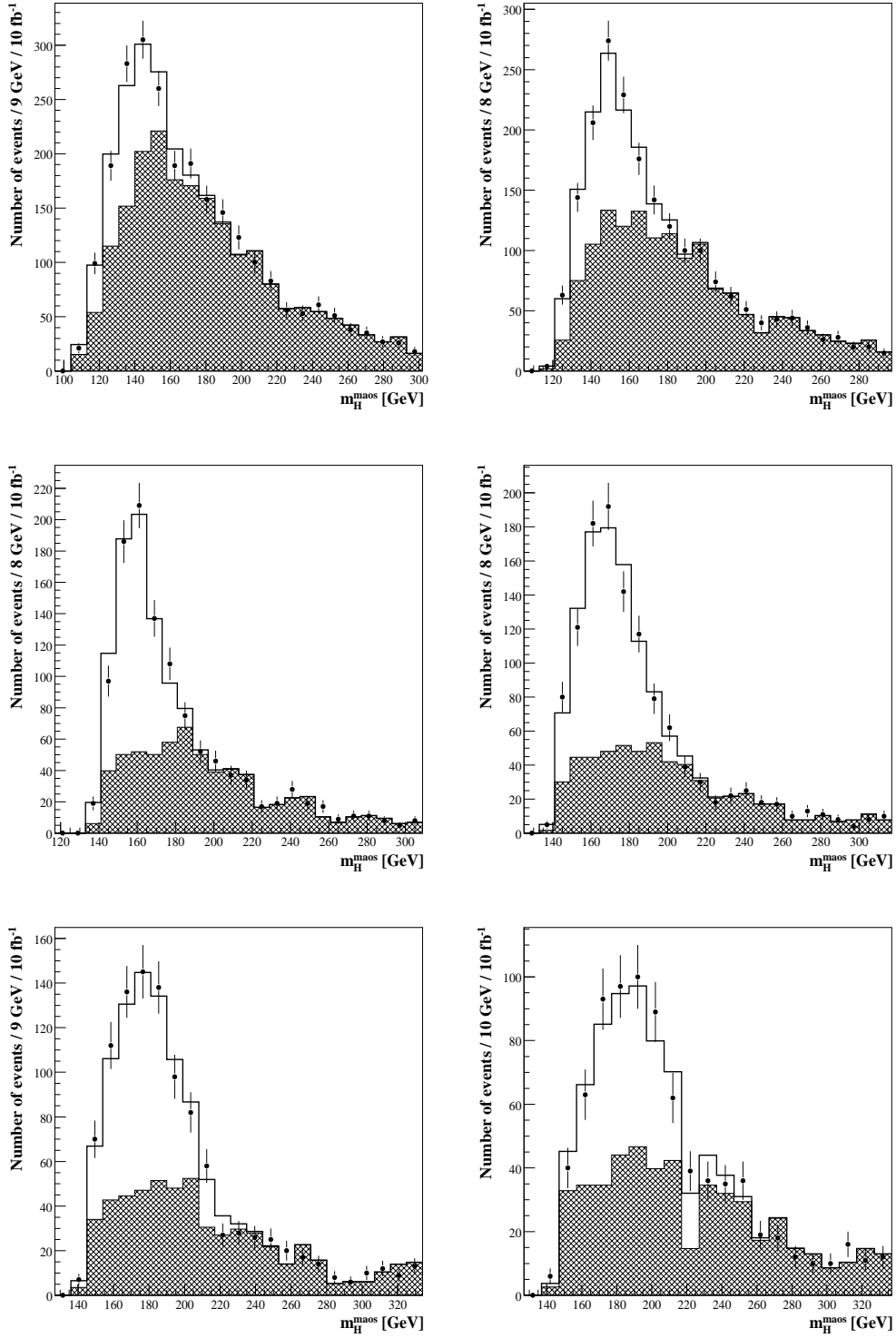


Figure 6: The m_H^{maos} distribution for the nominal data (dots) and the template (solid line) for various Higgs boson masses: $m_H = 140, 150, 160, 170, 180, 190$ GeV from the top left to the bottom right. In each frame, shaded region represents the backgrounds.

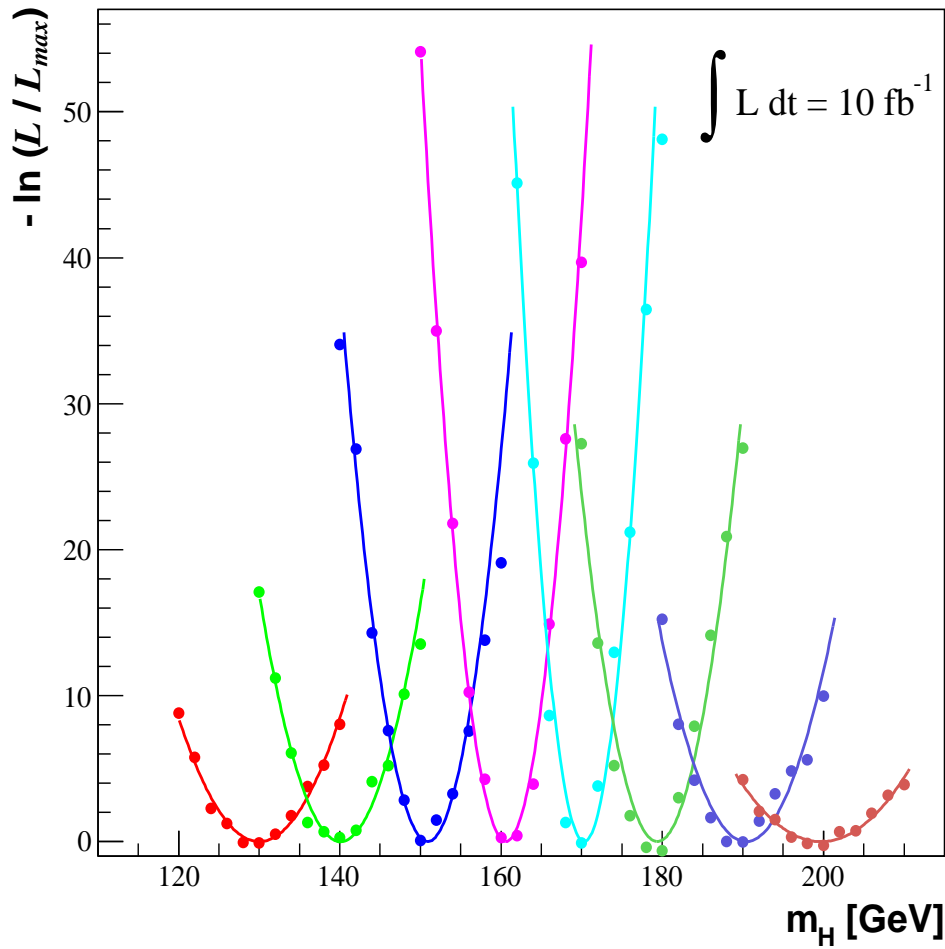


Figure 7: The relative log likelihood distributions for various Higgs boson masses. The solid line shows the result of the quadratic fitting for each value of m_H . The \mathcal{L}_{\max} is the maximum likelihood which was determined as the minimum of a fit to the $-\ln \mathcal{L}$ distribution.

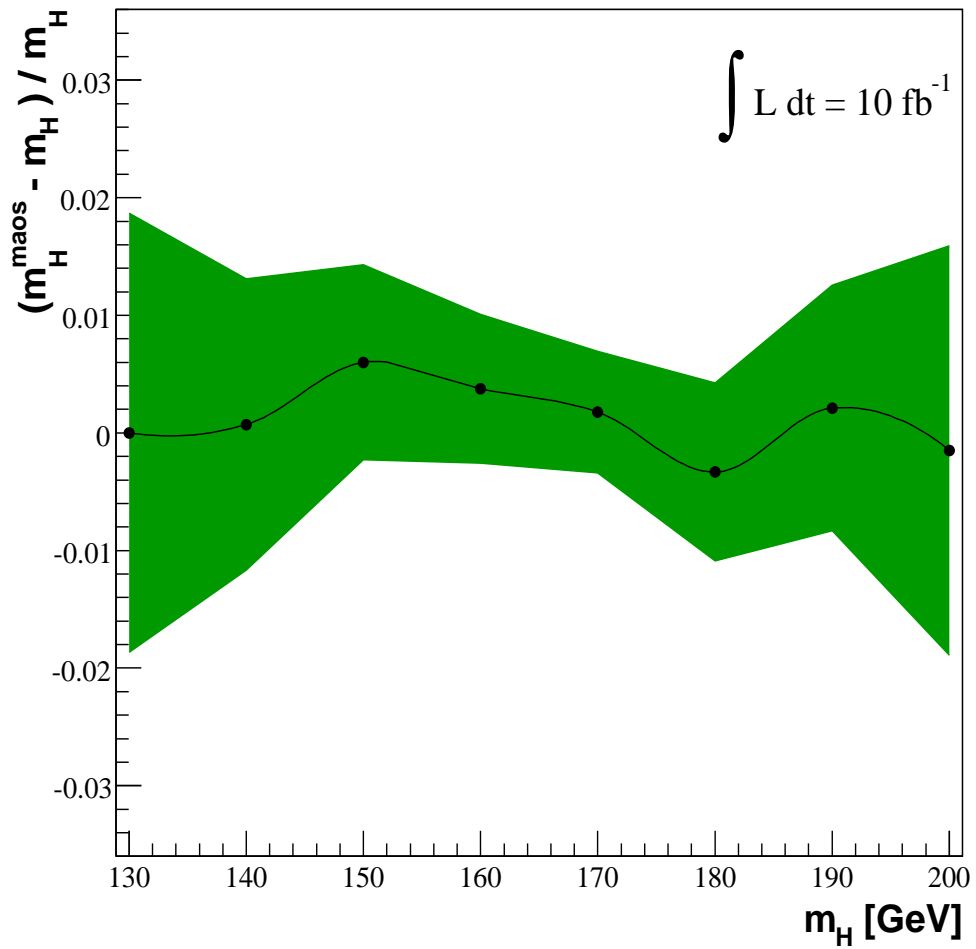


Figure 8: *The band showing the $1\text{-}\sigma$ deviation error for the Higgs boson mass determined by the m_H^{maos} distribution. The dots and lines denote the Higgs boson mass obtained by the likelihood fit.*